

# Dissolution Driven Fracture – Simulation of Crack Growth

C. Bjerken

Division of Materials Science  
Malmö University, Malmö Sweden  
e-mail: christina.bjerken@ts.mah.se

**Summary** The growth of a crack subjected to corrosion fatigue is studied using adaptive finite elements. The crack growth is the result of a repeated cycle of dissolution of the material, formation of a protective oxide film and break-down of the oxide film due to straining at the surface. The dissolution rate is assumed to be proportional to this stretching. The growth of a semi-infinite crack lying in an infinite strip subjected to different degrees of mixed-mode loading is studied.

## Introduction

During stress corrosion, loss of atoms to the environment leads to crack growth. This is a dissolution process that starts i.e. if bare metal is exposed to aggressive environments. Fortunately, an impermeable film of mainly metal oxides or hydroxides is formed by dissolved metal on several metals. Even though the thickness of this film is typically not more than 10 nm, it reduces the rate of dissolution by several orders of magnitude, cf. [1]. An intact protective film increases the life of the structure tremendously. However, repeated changes of the electrochemical conditions or cyclic mechanical load damage the film, which leads to additional material loss. Several experimental reports show that active loading in terms of either monotonically increasing or fatigue load is an essential prerequisite for development of corrosion cracks, cf. [2]. The passivating film is, as being an oxide or hydroxide compound, believed to have ceramic material properties. As such it is presumably brittle. Here it is supposed to fracture when stretched more than a threshold strain,  $\varepsilon_f$ .

If the threshold strain is exceeded, the film breaks and leave gaps where bare metal is exposed to the environment. The area extent of these gaps is assumed to be proportional to the strain exceeding the threshold strain. The broken film leaves gaps that give a discontinuous exposure to environment. In the present study, the dissolution rate is simply assumed to be proportional to the mechanical stretching of the body surface reduced with the threshold strain.

The film is known to be extremely thin as compared with the linear dimensions of the body. Therefore it is not contributing in any significant way to the structural stiffness. In the present analysis, the presence of the film, broken or unbroken, is ignored when the mechanical behaviour of the structure is computed.

The interacting dissolution and mechanical load leads to a roughening of the body surface, and, after localization, to initiation of corrosion pits. For large threshold strains, the pits assume the shape of cracks. These cracks are integral parts of the body surface. Growth rate and growth direction are results of the dissolution process. The model brings additional features to the crack tip in contrast to an assumed sharp crack tip, where the fracture processes are confined to a point and all the details of the crack tip state is given by a single parameter, such as a stress intensity factor or a crack tip driving force. This permits determination of the crack growth simply as the evolution of the body surface. Thus, crack growth criteria are not needed. Neither are crack path criteria needed, while also the direction of the crack extension results from dissolution rate along the body boundaries in the crack tip vicinity.

In the present study, crack paths are calculated using an adaptive finite element procedure. The strain concentration computed from the load and the geometry of the crack tip vicinity

predicts dissolution, i.e. removal of material and crack growth. The geometry is repeatedly re-meshed as the body shape is updated to accommodate the extending crack. The mesh maintains a resolution sufficient for a detailed calculation of the strain distribution in the crack tip region to ensure that the crack growth direction is accurately predicted.

Paths are found for a few cases involving different degrees of mixed mode loading. The results are compared with results for established crack path criteria.

### Computational method

In the present study, a computational method that evolves a body surface by an adaptive finite element procedure is used, cf. Jivkov [3]. The finite element code ABAQUS [4] is adopted for computing the strains along the surface. During loading, the oxide film is assumed to crack if the strain along the surface exceeds the threshold strain  $\varepsilon_f$ . This results in dissolution of material. Thus stretching of the body surface controls the rate of dissolution. A linear relation between the surface strain  $\varepsilon$  and the dissolution rate  $v$  is assumed:

$$v = C (\varepsilon - \varepsilon_f) \quad \text{for } \varepsilon > \varepsilon_f \quad (1)$$

where  $C$  is a constant depending only on the environment. The rate  $v$  is, in the present context, the linear extent per load cycle. The period of the load cycle is assumed to be long enough to allow full recovery of the protective oxide film. The electrochemical potential of the system is contained within  $C$ . The surface boundary is moved according to Eq. 1 along the normal direction of the surface. Because of the extremely small thickness of the oxide film, it is not included in the finite element model. Six-node triangular elements are used and re-meshing is done for each load cycle. Further details of the model cf. Jivkov [3]. The material is assumed linear elastic, and is subjected to fatigue loading under plane strain conditions.

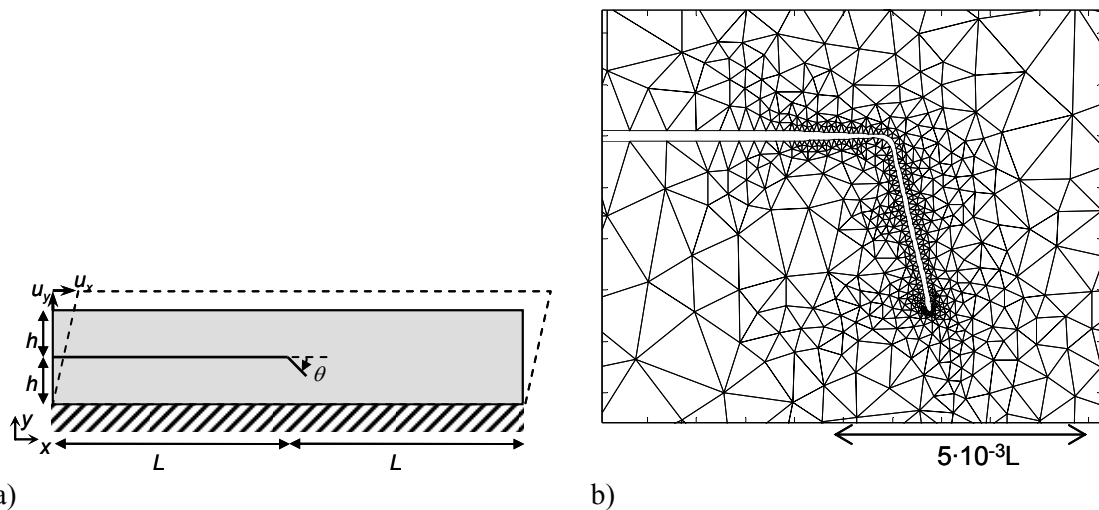


Figure 1. a) Geometry of the large strip used for the finite element analysis b) Mesh after 200 load cycles for a strip with global  $K_{II}$  load.

### Results

The crack propagation during is simulated for a semi-infinite crack in a strip, with the initial crack oriented parallel to the surface of the strip, loaded in different degrees of mixed mode. The

geometry used for the simulations are shown in Fig. 1.a. The length of strip is  $2L$  and the thickness  $2h$ , and the lower edge of the strip is allowed to move in the  $x$ -direction but is fixed in the  $y$ -direction. The load is applied at the upper edge as prescribed displacements  $u_x$  and  $u_y$ . The crack has an initial length  $L$  and it is located at  $y = h$ , between  $x = 0$  and  $L$ , with its tip at  $x = L$ . Simulations are performed for a few hundred cycles for eight different degrees of mixed mode loading. In Fig. 1.b, a typical finite element mesh is shown. Approximately 2000 elements are used during one load cycle, and the ratio of the largest and the smallest element sides is around 4000. The displacement ratio  $u_x/u_y$ , equals  $K_{II}/K_I$ , and the following ratios are investigated: 0, 0.2, 0.5, 1, 2, 5, 10 and  $\infty$ .

In Fig. 2.a, the crack paths after 200 load cycles for the investigated  $K_{II}/K_I$ -ratios are shown. The kinked part of a crack is approximately  $4 \cdot 10^{-3}L$ , the width of the crack is governed by the load and  $\varepsilon_f$ , cf. [3]. It can be seen that the larger the  $K_{II}$ , the more stable the shape of the crack. The crack driven by a global  $K_I$ -loading shows a tendency to branch at the crack tip. It can also be noted that for pure  $K_I$  global load the present method results in a crack path that is not horizontal initially. Though, after additionally a few hundred cycles this crack will flatten and find a path that is parallel with the initial crack.

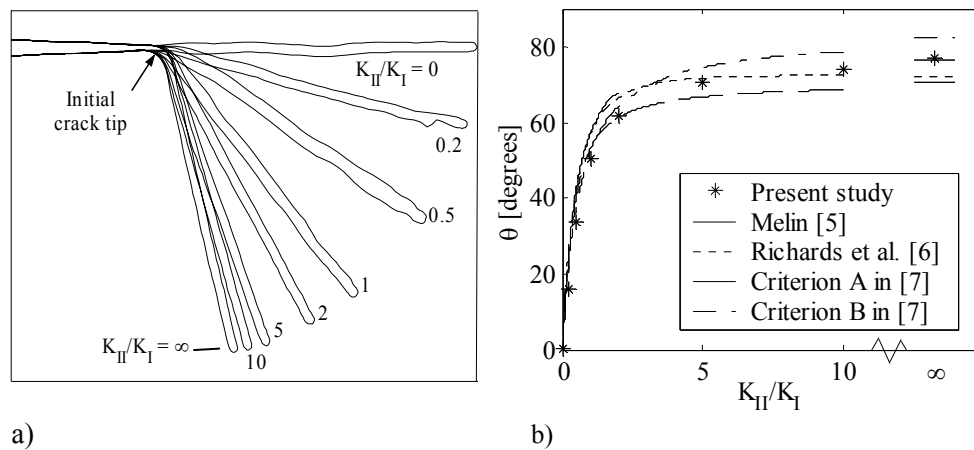


Figure 2.a) Crack paths for different  $K_{II}/K_I$ -ratios b) Kink angles versus  $K_{II}/K_I$  for different criteria

The kink angle,  $\theta$ , is measured to the centre line of the crack, and the values are plotted in Fig. 2.b. These results are compared to kink angles obtained by four different crack paths criteria for sharp cracks found in the literature. Melin [5] computed kink angles by maximizing the local mode I stress intensity factor,  $k_I$ , at the tip of an infinitesimal kink of a sharp crack. Richard et al. [6] use a criterion based on a numerical adoption to experimental findings. Additionally, two of the criteria studied by Bergqvist and Guex [7] are used for comparison; the criteria of maximum principle stress by Erdogan and Sih [8] (Criterion A) and of the maximum J-integral by Sih [9] (Criterion B). All criteria give similar results as in the present study. For dominating global  $K_{II}$  loading, i.e.  $K_I=0$ , the hypothesis of maximum  $k_I$  shows best agreement.

## Discussion

The present method is based on the calculations of strains along the parts of a body that are assumed to be in contact with a corrosive media. The tip of the resulting crack has a finite geometry as opposed to conventional methods where it is treated as a single point. The part of the crack tip region that exceeds the threshold strain for oxide film breakage will dissolve and the

crack grows by evolving the surface of the body. During crack growth local broadening of the crack tip region will develop, which in turn can induce crack branching.

### Conclusions/Concluding remarks

In the present study, it is shown that crack paths can be followed without criteria for neither crack growth nor crack path. An adaptive finite element procedure was used to simulate the moving boundary of a body subjected to strain driven corrosion fatigue.

Results for kink angles due to mixed mode loading of a crack computed with the presented criteria free method was found to agree well with predictions from criteria for sharp cracks found in the literature. The best agreement was found for dominating global  $K_{II}$  loading, while for dominating  $K_I$  loading the deviation was larger.

It is believed that the criterion free method can be a plausible choice for studying situations where criteria for crack growth, crack branching and crack path criteria fail, e.g. interface cracks, crack initiation from notch or surface and meeting cracks.

### References

- [1] Smallman, R.E. and Bishop, R.J. *Modern Physical Metallurgy Materials Engineering*, 6<sup>th</sup> ed, pp. 376-387, Butterworth-Heinemann, Avon, UK, (1999).
- [2] Jones, R.H., and Ricker, R.E., *Stress-Corrosion Cracking*, pp. 1-39, Jones, R.H. (Ed.) ASM International, USA, (1992).
- [3] Jivkov, A., *Strain-assisted corrosion cracking and growth rate inhibitors*, PhD thesis, Lund University, Sweden, (2002).
- [4] *ABAQUS User's manual*, Version 6.4, Abaqus Inc. ,(2004).
- [5] Melin, S., Fracture from a straight crack subjected to mixed mode loading, *Int. J. Fract. Mech.* **32**, 257-263, (1987).
- [6] Richard, H.A., Fulland, M. and Sander, M., Theoretical crack path prediction, *Fatigue Fract. Engng Mater. Struct.* **28**, 3-12, (2005).
- [7] Bergkvist, H. and Guex, L., Curved crack propagation, *Int. J. Fract.* **15**, 429-441, (1979).
- [8] Erdogan, F. and Sih, G.C., On the crack extension in plates under plane loading and transverse shear, *J. Basic Engng*, **85**, 519-527, (1963).
- [9] Sih, G.C., Strain energy density factor applied to mixed mode crack problems, *Int. J. Fract.*, **10**, 305-321, (1974).